CHEMISTRY
A EUROPEAN JOURNAL

DOI: 10.1002/chem.201000330

Ultrafast Synthesis of Layered Titanate Microspherulite Particles by Electrochemical Spark Discharge Spallation

Yuxin Tang,[a] Yuekun Lai,[a, b] Dangguo Gong,[a] Kok-Hui Goh,[c] Teik-Thye Lim,[c] Zhili Dong,*[a] and Zhong Chen*[a]

Recently, a new hydrothermal approach to fabricate titanate materials has attracted much attention.[1] These layered titanate nanomaterials show excellent abilities in ion-exchange, absorption, photoelectronicity, and so on.[2] To satisfy the requirement of different applications, there has been a drastic increase in research to develop new approaches to produce different types of semiconductor oxide nanostructures, especially titanium-based oxides. Up to now, the synthesis of 1D and 2D nanotitanate has been widely investigated with many interesting properties reported. For example, 1D titanate nanotubes, nanowires, nanorods, and 2D titanate nanosheets have been synthesized by hydrothermal, high-temperature oxidation, molten-salt synthesis, and exfoliation methods.[3] Among which hydrothermal synthesis is most widely used.[2e,3] Recent investigations have demonstrated that 3D hierarchical nanostructures could improve the performance of the material in catalysis, biomedical, energy conversion, and water-treatment applications, among others, due to the superior properties derived from the high specific surface area and porous structure.[4] However, it is still challenging to produce 3D hierarchically complex shapes of titanate over multiple scales and the synthetic method is usually not straightforward.[5] Until now, the general approach for preparing hierarchical titanate structures involved the use of sacrificial templates, such as zinc oxide nanotemplate.[5a] Alternatively, the template-free methods for generating hierarchical titanates typically employ bottom-up methods, such as reacting agar gel containing a solution of titanium precursor in NH_4OH,[5b] two-stage growth through an H_2O_2-enhanced oxidation process,[5c] two-step synthesis combining hydrolysis and hydrothermal treatment,[5d] the chimie douce route by heating TiO_2 powder in 15 M NaOH solution at reflux,[5e] and self-assembly by treating $TiCl_4$ precursor in ethylenediamine at high temperatures.[5f] These approaches either take multiple steps or require a long time to ensure complete reaction, for example, the time taken for the reaction between agar gel with Ti precursor and NH_4OH is one week.[5b] A simple, fast, and inexpensive method to form 3D hierarchical nanostructures is still lacking and will be of great interest.

It is known that a TiO_2 porous layer can be formed on a Ti foil surface by mild anodic oxidation in fluoride-containing solutions, rapid breakdown anodization in chloride-/perchlorate-containing electrolytes, or a plasma electrolytic oxidation method.[6] However, to the best of our knowledge, there are no reports using these techniques to generate the titanate materials in powder form, which is traditionally prepared by hydrothermal method.[3,5] Herein, we report a one-step, template-free method (electrochemical spark discharge spallation) to quickly fabricate layered titanate hierarchical microspherulites (TMSs) with a large surface area ($406\ m^2 g^{-1}$) by carefully adjusting the applied electrical spark parameters in the experimental setup (Figure S1 in the Supporting Information). The formation principle of the layered titanate is different from the formation of the TiO_2 nanostructures, which include two important steps. First, an ultrahigh anodic reaction oxidizes the Ti surface layer and the formed oxide is immediately broken down by the applied electrical field into the solution in the form of small precipitates. This spallation of the oxide particle is driven by the continuously discharged sparks that simultaneously heat

[a] Y. Tang, Dr. Y. Lai, D. Gong, Prof. Z. Dong, Prof. Z. Chen
School of Materials Science and Engineering
Nanyang Technological University, 50 Nanyang Avenue
639798 (Singapore)
Fax: (+65) 6790-9081
E-mail: zldong@ntu.edu.sg
aszchen@ntu.edu.sg

[b] Dr. Y. Lai
State Key Laboratory of Physical Chemistry of Solid Surfaces
College of Chemistry and Chemical Engineering
Xiamen University, Xiamen, 361005 (China)

[c] K.-H. Goh, Prof. T.-T. Lim
School of Civil and Environmental Engineering
Nanyang Technological University, 50 Nanyang Avenue
639798 (Singapore)

Supporting information for this article is available on the WWW under http://dx.doi.org/10.1002/chem.201000330.

up the solution. Second, the precipitates immediately react with the hot NaOH solution to form the TMS particles. The total reaction is within 20 min. Also, this method is different from all known approaches to form titanate nanostructure. For example, Ti foils could be hydrothermally treated to form titanate nanotube or wires on its surface. However, there were few titanate precipitates in the solution even at high temperatures inside an autoclave.[7]

A typical FESEM and TEM image of the TMS formed in 10 M NaOH for 20 min is shown in Figure 1a and b, respectively. It is observed that the as-prepared TMSs are well dispersed and the particle sizes range from 0.4 to 1.5 μm. The inset image in Figure 1a shows that densely populated titanate nanoribbons (TNRs) radiate from the core of the TMS. The TEM image in Figure 1b reveals that the 3D hierarchical TMS is highly porous. The surface area of the as-prepared TMS is 406 $m^2 g^{-1}$ (Figure S2 in the Supporting Information), which is higher than the reported values of titanate spheres[5e] and nanotubes.[3h] From the high-resolution TEM fringes in Figure 1c, the interlayer distance of the layered TNRs is approximately 0.75 nm, which is smaller than the result obtained from the XRD measurement, with a *d* spacing of 0.96 nm (Figure 1d). This deviation is caused by the dehydration of the titanate in ultrahigh vacuum during the TEM observation, which has been reported in previous work.[5a,b] The diffraction pattern of the TMS powder indicates that the product has an orthorhombic $H_2Ti_2O_5 \cdot H_2O$ (JCPDS no. 47-0124) layered crystal structure. The broad peaks at $2\theta = 9.2$ (d = 0.96), 24.6 (d = 0.36), 28.5 (d = 0.31), 34.9 (d = 0.26), 38.8(d=0.23), 48.3 (d = 0.19), and 62° (d = 0.15 nm) correspond to the (200), (110), (310), (301), (501), (020), and (002) planes. Such a crystal structure consists of similar lepidocrocite-type host layers (inset of Figure 1d) to those in the layered $H_{0.7}Ti_{1.825}\Delta_{0.175}O_4 \cdot H_2O$ (Δ: vacancy), but with different protons.[3f,g,h] The inset of Figure 1b is the electron diffraction pattern of TMS. Diffraction rings are observed because the sample is polycrystalline with nanoribbons radiating outwards. The three diffraction rings are indexed as the three intensive (110), (310), and (020) diffraction planes for the orthorhombic titanate, which is consistent with the XRD result.

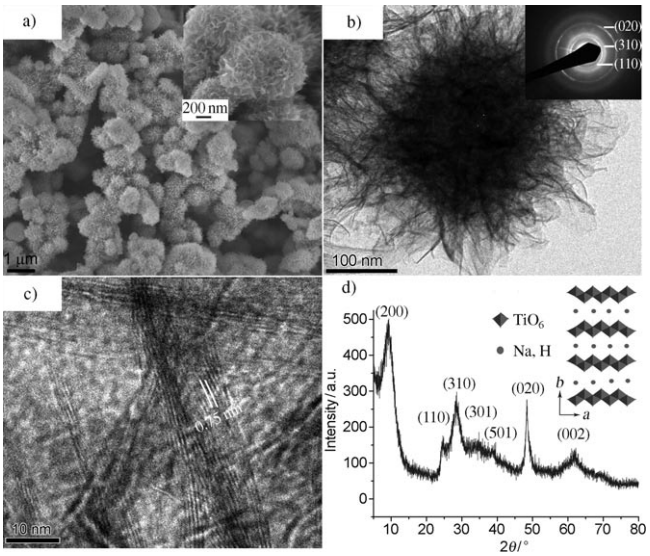

Figure 1. a) FESEM image, b) TEM image, c) high-resolution TEM image, and d) XRD pattern of the fabricated TMS The insets in a) and b) are the magnified image and electron diffraction pattern of TMS. The inset in d) shows the crystal structure for lepidocrocite titanates. The TMS powder is collected after anodization of Ti foils in a 10 M aqueous solution of NaOH for 20 min.

Figure 2 shows the anodic voltage and solution temperature versus time behavior observed at a constant current density of 0.5 $A cm^{-2}$. Raman scattering spectra of the powders produced at different stages is shown in the inset. The voltage plot exhibits two distinct regions: i) an initial abrupt increase to a maximum followed by ii) a rapid decrease to a steady state. The steady state in the voltage indicates the equilibrium between the formation and spallation of the anodized titanium oxide layer on Ti foil surface. Meanwhile, the solution temperature increases gradually with the time and finally reaches a steady state around 110 °C. Formation mechanism of TMSs consisting of TNRs can be explained in the light of the voltage and temperature versus time plots as follows: The formation of TMS powder involves two processes composed of electrochemical anodization and reaction of the anodized precipitates with the electrolyte solution. Initially, Ti oxidizes to form a compact TiO_2 layer on the Ti foil surface by the reactions shown for the anode in Equation (1) and the anode and solution shown in Equation (2).

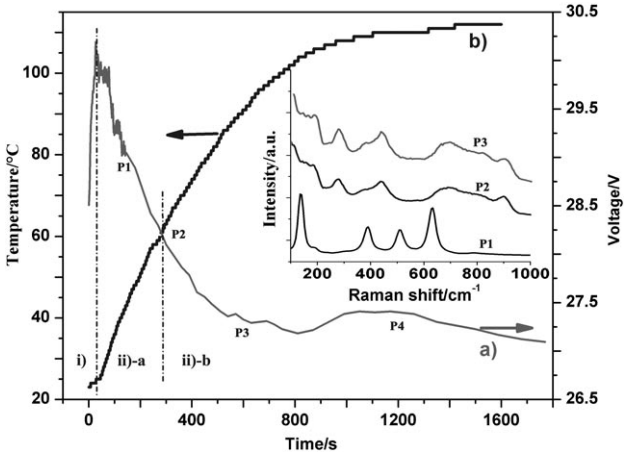

Figure 2. Real-time observation of anodization voltage (a) and solution temperature (b) of Ti foil anodized at a constant current density of 0.5 $A cm^{-2}$ in a 10 M aqueous solution of NaOH. Inset shows Raman scattering spectra of the powders collected from the solution at different durations marked on the plot. The regions i), ii)-a and ii)-b show the different stages of the spark discharge process.

$$Ti - 4e \rightarrow Ti^{4+} \quad (1)$$

$$Ti^{4+} + 4OH^- \rightarrow TiO_2 \cdot 2H_2O \quad (2)$$

The thickening of the oxide layer with increasing reaction results in an increase in anode resistance, leading to the dramatic increase of the anode voltage (Figure 2, region i). Simultaneously, a rapid evolution of hydrogen at the cathode is observable as strong bubbling due to reaction shown in Equation (3):

$$2H^+ + 2e \rightarrow H_2 \uparrow \quad (3)$$

We find that in the current setup, the applied voltage (≈27.1 to 30.3 V, Figure 2) is more than the TiO_2 breakdown voltage (about 25 V) in a 10 M aqueous solution of NaOH. Thus, the oxide layer at the electrolyte/oxide interface is electrically broken down and spalled into the solution in the form of small precipitates by the generated spark discharge. On the Ti surface, corresponding pits are observed (Figure S3 in the Supporting Information). In region ii)-a of Figure 2, as the anodization proceeds, the oxide layer starts to dissolve with numerous small pores on its surface (Figure S4a-b in the Supporting Information), which leads to the observed rapid decrease in the voltage. The anodization spark spallation loop is a continuous process, generating a large quantity of TMS in the solution. Moreover, the anodization spark spallation process can induce the formation of crystalline TiO_2 structure, which is triggered by the local exothermic heat caused by the vigorous spark discharge. The Raman data shown in the inset of Figure 2 (point P1) suggests that the precipitate is anatase because of the bands located at 144, 198, 398, 515, and 640 cm^{-1} belonging to Raman active modes ($A_{1g}+2B_{1g}+3E_g$) of the anatase phase.[3h] The morphology of the TiO_2 precipitate is composed of microscale sphere- and stem-like structures, and the surface of precipitate is porous (Figure 3a). The TEM image shown in Figure 3b reveals that the spherulite surface consists of small ribbons, while the core remains solid. In region ii)-b of Figure 2, the hydrothermal reaction takes place in solution due to the increase of solution temperature, as shown in Equation (4).

$$2\,TiO_2 + 2\,NaOH \rightarrow Na_2Ti_2O_5 \cdot H_2O \quad (4)$$

Figure 3c, corresponding to the point P2 on the plot given in Figure 2, shows that the average size of precipitates decreases compared with that shown in Figure 3a for point P1 (Figure 2). This is likely to be due to the decrease of the critical breaking-down thickness of the TiO_2 layer in a heated solution in which the voltage applied to the dielectric layer decreases. The titania–titanate transformation thoroughly takes place in small particles, which means that the whole spherulite only consists of the radiating nanoribbons (Inset of Figure 3d). For large particles, only the outer layer is covered with nanoribbons (Figure 3d). The broad Raman bands located near 188, 280, 389, 447, 705, and 905 cm^{-1} belong to titanate structure[3h] when the sample is collected at points P2 and P3 (Figure 2), indicating that the anatase TiO_2 precipitates have been transformed into TNRs in region ii)-b when the solution temperature is greater than 60 °C. The formation of TNR is due to the dissolution/crystallization of the TiO_2 at high alkaline conditions at relatively low solution temperatures (<130 °C), and it is an observed intermediate product of nanotube/wire formed at high temperatures.[2,5a–b] As the reaction proceeds (P3, Figure 2), the retrieved particles almost completely consist of nanoribbons (Figure 3e–f), which means the reaction extends to the whole precipitate. Some of these completely reacted particles can be observed on the Ti foil surface too (Figure S4c-d in the Supporting Information). Further extended treatment at P4 (Figure 2) sees similar morphology (Figure 1a, b) and Raman spectra with P3, which indicates a steady state has been reached beyond 20 min of reaction.

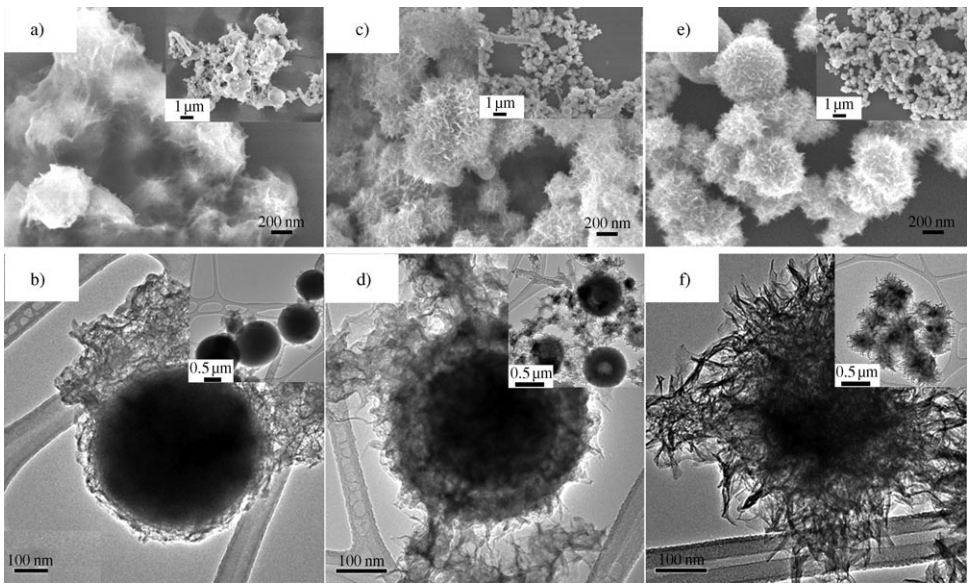

Figure 3. FESEM (a, c, e) and TEM (b, d, f) images of powder samples taken at points marked P1 (a, b), P2 (c, d), and P3 (e, f) in Figure 2. The inset images are the same samples taken at low magnification.

Recent work reveals that the titanate materials show excellent ion-exchange ability for the removal of toxic radioactive and heavy-metal ions, which are very harmful to living organisms.[2a,b] Divalent lead (Pb^{II}), one of the metals that has the most damaging effects on human health, can cause damage to the central nervous system and dysfunction to the kidneys and immune system of human beings, especially in children.[8] Herein, we investigate the ability of our 3D TMS to absorb toxic heavy-metal Pb^{II} ions and methylene blue (MB), an organic dye. Figure 4

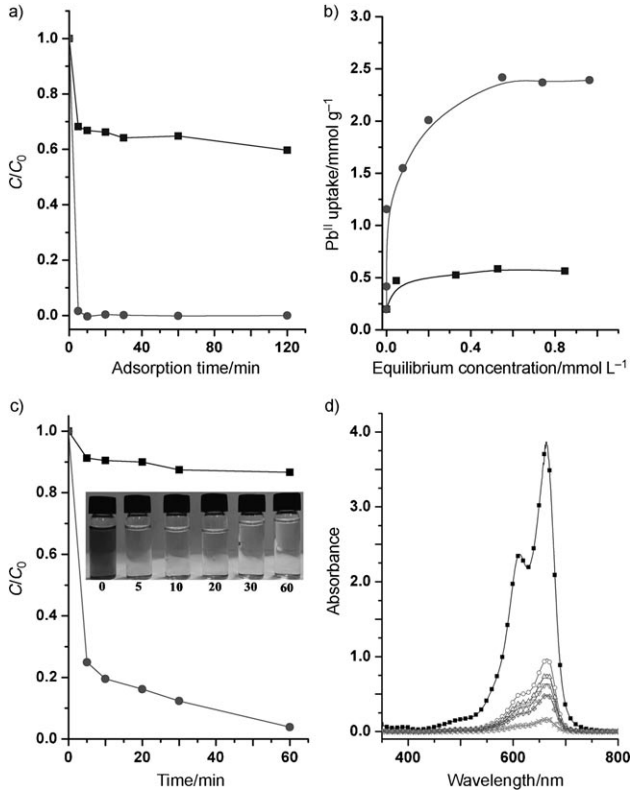

Figure 4. Comparison of a) adsorption rate ($C_o = 120.52\ mg\,L^{-1}$) and b) adsorption isotherms of Pb^{II} adsorption; c) adsorption rate ($C_o = 20\ mg\,L^{-1}$) of MB adsorption by pyrosynthesized trititanate particles (■) and anodized TMS (●); d) absorption spectra of MB solution in the presence of new hierarchical TMS at 0 (■), 5 (○), 10 (△), 20 (▽), 30 (◇), and 60 min (×). Inset of c shows photos of absorption of MB with time by hierarchical TMS. C_o and C are the initial concentration and the concentration of the Pb^{II} or MB solution after adsorption at different intervals, respectively.

shows the absorption of Pb^{II} and MB dye in an aqueous solution. Details of the adsorption experiment are given in the Supporting Information. For comparison, we also synthesized micro-sized sodium trititanate by a high-temperature, solid-state reaction (Figure S5 in the Supporting Information). Our TMS is able to remove Pb^{II} from the solution almost completely in less than 10 min, as evidenced by the concentration decrease from $120.52\ mg\,L^{-1}$ (C_o) to less than $0.5\ mg\,L^{-1}$ at room temperature. The trititanate formed by the pyrosynthesis method shows only very limited absorption. Moreover, the adsorption rate of our TMS particles is far higher than trititanate particles. Table S1 in the Supporting Information lists the reported removal capacity values from existing reports, and our TMS is the best ($2.41\ mmol\,g^{-1}$) without any further optimization. Our TMS also shows a high adsorption rate (Figure 4c and d, $C_o = 20\ mg\,L^{-1}$) and excellent adsorption capacity of MB dye (Figure S6 in the Supporting Information). This excellent adsorption performance is due to the unique hierarchical structure and crystal structure of the as-prepared TMS. The isolated nanoribbon structure gives rises to the large surface area, which is the prevailing factor for the fast MB removal rate and capacity. Moreover, the removal of Pb^{II} ions is an ion-exchange process, in which the exchange capacity is the key parameter.[2a] The obtained TMS has the chemical formula $A_2Ti_2O_5$ (A = Na, H) with a theoretical cation-exchange capacity of $9.05\ mmol\,g^{-1}$, whereas that for trititanate $Na_2Ti_3O_7$ is $6.62\ mmol\,g^{-1}$. Therefore, the surface area and the crystal structure are the main factors that give rise to the excellent adsorption rate and capacity of our TMS particles.

In summary, we have demonstrated a new template-free method that utilizes rapid electrochemical anodization and electrical discharge spallation to synthesize 3D hierarchical TMS particles with a large surface area in an ambient setup. The mechanism for the formation of the particles and their hierarchical structures has also been proposed. The obtained TMS powders show excellent adsorption ability and a high adsorption rate for toxic Pb^{II} ions and the MB dye due to their specific morphology and crystal structures. We expect a wide range of applications for this type of material or its derivatives, such as in photocatalysis or lithium batteries.

Experimental Section

Preparation: As shown in Figure S1 in the Supporting Information, the Ti foil (99.7% purity purchased from Aldrich Corporation, $2\ cm^2$, anode) was subjected to galvanostatic anodization current ($0.5\ A\,cm^{-2}$) in a two-electrode electrochemical cell connected to a DC power supply. A platinum foil (99.9% purity, 2.5×1.5 cm) served as the counter electrode. The electrochemical spark discharge process should be carried out in a fume hood with good ventilation so that any generated gases can be instantly removed. The experiments were conducted in 10 M aqueous solutions of NaOH (≈60 mL) under ambient conditions (≈25 °C) for 20 min without any heating or stirring. The solution temperature increased to about 110 °C at the end of reaction. When the solution cooled to room temperature, the grey/white precipitate (≈0.25 g) collected from the solution was centrifuged and then washed with deionized water three times to yield the TMSs.

Characterization: The morphology of the as-synthesized 3D TMS was investigated by using FESEM (JEOL, JSM-6340F instrument). For TEM observation, the suspension was dropped onto a copper grid and dried at room temperature. A transmission electron microscope (JEOL, JEM-2010) operating at 200 kV was used to characterize the nanostructures. A Shimadzu 6000 X-ray diffractometer with a $Cu_{K\alpha}$ source was used for phase identification. Nitrogen adsorption/desorption isotherms were measured at 77 K using ASAP2000 adsorption apparatus from Micromeritics. The samples were degassed at 100 °C for 4 h under vacuum before analysis. Raman measurements were performed at room temperature in a WITEC confocal spectrometer with a 488 nm excitation laser operated at a low power level (1 mW), and the Si peak ($520\ cm^{-1}$) was used as a reference for wavenumber calibration.

Acknowledgements

The authors thank the National Research Foundation of the Singapore Government (Grant MEWR651/06/160) for their financial support.

Keywords: electrochemistry · hydrothermal synthesis · layered compounds · nanoparticles · titanates

[1] T. Kasuga, M. Hiramatsu, A. Hoson, T. Sekino, K. Niihara, *Langmuir* **1998**, *14*, 3160–3163.

[2] a) D. J. Yang, Z. F. Zheng, H. Y. Zhu, H. W. Liu, X. P. Gao, *Adv. Mater.* **2008**, *20*, 2777–2781; b) D. J. Yang, Z. F. Zheng, H. W. Liu, H. Y. Zhu, X. B. Ke, Y. Xu, D. Wu, Y. Sun, *J. Phys. Chem. C* **2008**, *112*, 16275–16280; c) X. M. Sun, Y. D. Li, *Chem. Eur. J.* **2003**, *9*, 2229–2238; d) A. Riss, M. J. Elser, J. Bernardi, O. Diwald, *J. Am. Chem. Soc.* **2009**, *131*, 6198–6206; e) D. V. Bavykin, J. M. Friedrich, F. C. Walsh, *Adv. Mater.* **2006**, *18*, 2807–2824; f) Y. Lai, Y. Chen, Y. Tang, D. Gong, Z. Chen, C. Lin, *Electrochem. Commun.* **2009**, *11*, 2268–2271.

[3] a) T. Sasaki, M. Watanabe, *J. Am. Chem. Soc.* **1998**, *120*, 4682–4689; b) N. Miyamoto, H. Yamamoto, R. Kaito, K. Kuroda, *Chem. Commun.* **2002**, 2378–2379; c) Z. Liu, T. Yamazaki, Y. Shen, D. Meng, T. Kikuta, N. Nakatani, *J. Phys. Chem. C* **2008**, *112*, 4545–4549; d) C. C. Tsai, H. S. Teng, *Chem. Mater.* **2006**, *18*, 367–373; e) Q. Chen, W. Z. Zhou, G. H. Du, L. M. Peng, *Adv. Mater.* **2002**, *14*, 1208–1211; f) C. Y. Xu, Q. Zhang, H. Zhang, L. Zhen, J. Tang, L. C. Qin, *J. Am. Chem. Soc.* **2005**, *127*, 11584–11585; g) R. Z. Ma, Y. Bando, T. Sasaki, *Chem. Phys. Lett.* **2003**, *380*, 577–582; h) T. Gao, H. Fjellvag, P. Norby, *Inorg. Chem.* **2009**, *48*, 1423–1432.

[4] a) J. S. Hu, L. S. Zhong, W. G. Song, L. J. Wan, *Adv. Mater.* **2008**, *20*, 2977–2982; b) F. M. Zhan, B. Y. Geng, Y. J. Guo, *Chem. Eur. J.* **2009**, *15*, 6169.

[5] a) J. Q. Huang, Z. Huang, W. Guo, M. L. Wang, Y. G. Cao, M. C. Hong, *Cryst. Growth Des.* **2008**, *8*, 2444–2446; b) Y. Takezawa, H. Imai, *Small* **2006**, *2*, 390–393; c) Y. B. Mao, M. Kanungo, T. Hemraj-Benny, S. S. Wong, *J. Phys. Chem. B* **2006**, *110*, 702–710; d) J. Jitputti, T. Rattanavoravipa, S. Chuangchote, S. Pavasupree, Y. Suzuki, S. Yoshikawa, *Catal. Commun.* **2009**, *10*, 378–382; e) C. W. Peng, T. Y. Ke, L. Brohan, M. Richard-Plouet, J. C. Huang, E. Puzenat, H. T. Chiu, C. Y. Lee, *Chem. Mater.* **2008**, *20*, 2426–2428; f) C. Wu, L. Lei, X. Zhu, J. Yang, Y. Xie, *Small* **2007**, *3*, 1518–1522.

[6] a) G. K. Mor, O. K. Varghese, M. Paulose, K. Shankar, C. A. Grimes, *Sol. Energy Mater. Sol. Cells* **2006**, *90*, 2011–2075; b) A. Ghicov, P. Schmuki, *Chem. Commun.* **2009**, 2791–2808; c) R. Hahn, T. Stergiooulus, J. M. Macak, D. Tsoukleris, A. G. Kontos, S. P. Albu, D. Kim, A. Ghicov, J. Kunze, P. Falaras, P. Schmuki, *Phys. Status Solidi RRL* **2007**, *1*, 135–137; d) K. Shankar, J. I. Basham, N. K. Allam, O. K. Varghese, G. K. Mor, X. J. Feng, M. Paulose, J. A. Seabold, K. S. Choi, C. A. Grimes, *J. Phys. Chem. C* **2009**, *113*, 6327–6359; e) A. L. Yerokhin, X. Nie, A. Leyland, A. Matthews, S. J. Dowey, *Surf. Coat. Technol.* **1999**, *122*, 73–93; f) F. C. Walsh, C. T. J. Low, R. J. K. Wood, K. T. Stevens, J. Archer, A. R. Poeton, A. Ryder, *Trans. Inst. Met. Finish.* **2009**, *87*, 122–135.

[7] a) Y. Guo, N. H. Lee, H. J. Oh, C. R. Yoon, K. S. Park, H. G. Lee, K. S. Lee, S. J. Kim, *Nanotechnology* **2007**, *18*, 295608; b) Y. H. Wu, M. C. Long, W. M. Cai, S. D. Dai, C. Chen, D. Y. Wu, J. Bai, *Nanotechnology* **2009**, *20*, 185703.

[8] a) M. R. Huang, Q. Y. Peng, X. G. Li, *Chem. Eur. J.* **2006**, *12*, 4341–4350; b) X. J. Ju, S. B. Zhang, M. Y. Zhou, R. Xie, L. Yang, L. Y. Chu, *J. Hazard. Mater.* **2009**, *167*, 114–118.

Received: February 7, 2010
Published online: June 8, 2010

